

Electronic Supplementary Information

Superlow load of nanosized MnO on the porous carbon matrix from wood fibre with superior lithium ion storage performance

Chunxiao Yang,^a Qiuming Gao,^{a*} Weiqian Tian,^a Yanli Tan,^a Tao Zhang,^b Kai Yang^a and Lihua Zhu^a

Preparation of the MnO/C with different contents of MnO:

China fir (CF) was air dried with the water content lower than 20 wt.%. The CF xylem fibres were smashed and sieved to powder. 1.00 g of the CF powder was washed three times in deionized water to remove the dissolved impurity. To prepare MnO/C nanocomposite materials with different MnO contents, different amounts of KMnO₄ and Na₂SO₄, including 0.02 g KMnO₄ and 0.02 g Na₂SO₄ for MnO/C-1.9, 0.035 g KMnO₄ and 0.035 g Na₂SO₄ for MnO/C-3.2 and 0.09 g KMnO₄ and 0.09 g Na₂SO₄ for MnO/C-8.9, were dispersed into distilled water. The CF powders were added into the above precursor solutions and stirred for 1 h at room temperature. After soaked, the brown precipitates were filtered and washed and dried at 60°C for 12 h in an oven. In order to obtain MnO/C composite materials, the as-prepared precursor samples were placed inside an alumina boat in dimethylformamide and heated in a tube furnace to 600°C at a rate of 2°C min⁻¹ and kept for 4 h under a flowing N₂ atmosphere.

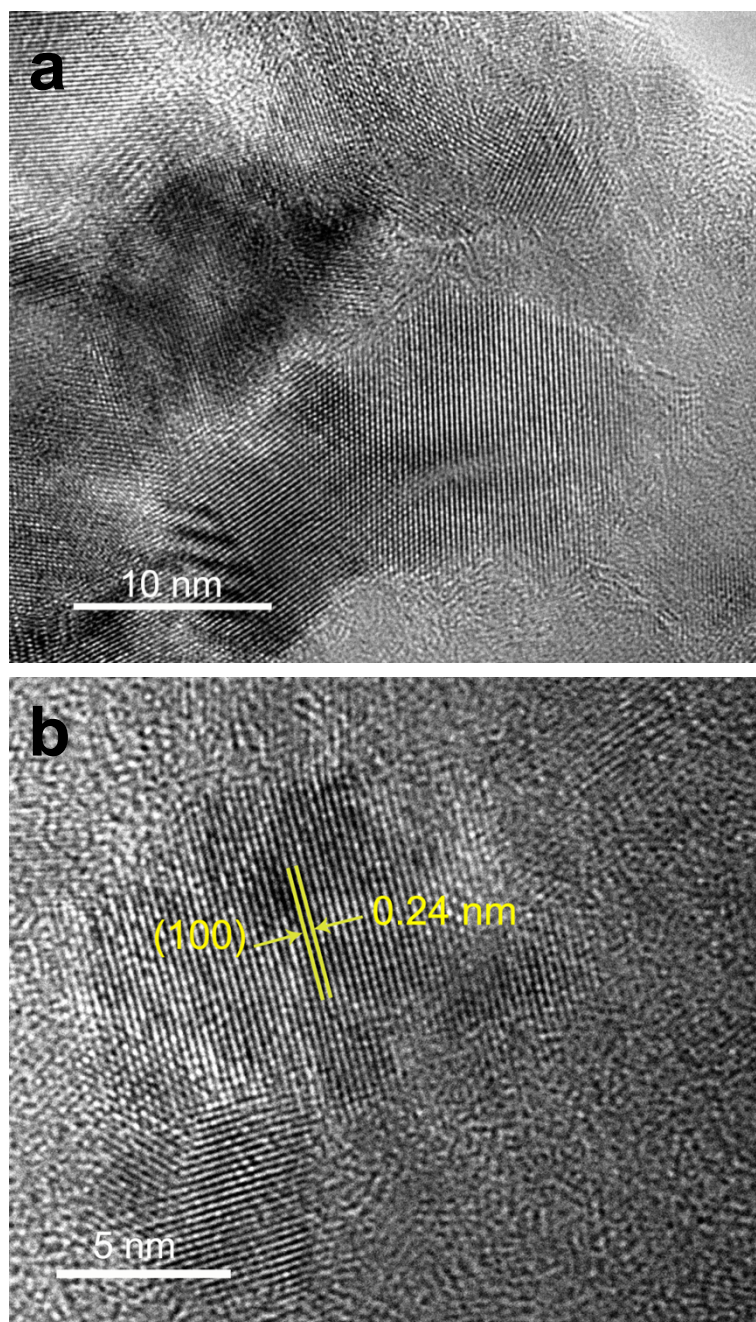
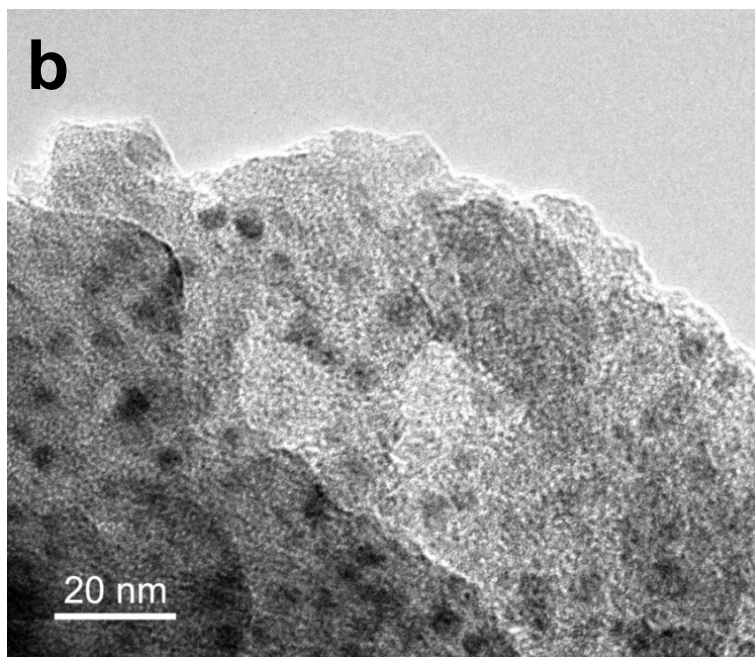
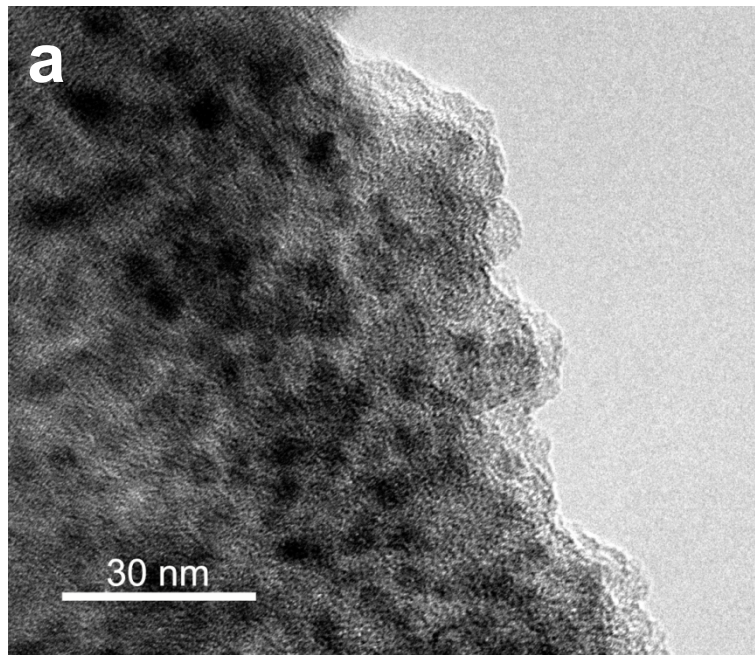


Figure S1: (HE)TEM images of the MnO₂/CF precursor with different enlargements (a and b). The periodic lattice fringe with distinct interplanar distance of 0.24 nm corresponding to the (100) plane of MnO₂ (JCPDS No. 42-1169) (b).



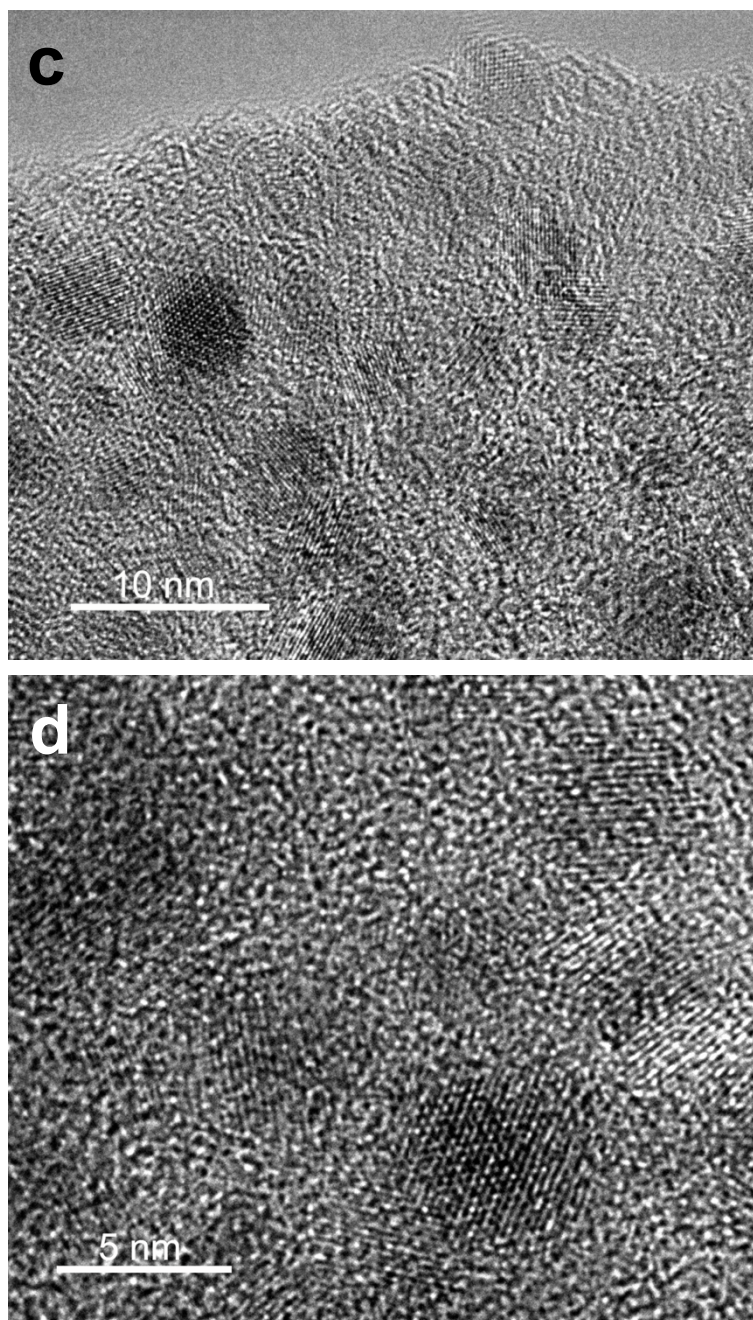


Figure S2: (HR)TEM images of the MnO/C sample with different enlargements (a-d). The well-crystallized MnO nanoparticles with diameters ranging from 3 to 7 nm are evenly dispersed on the carbon matrix.

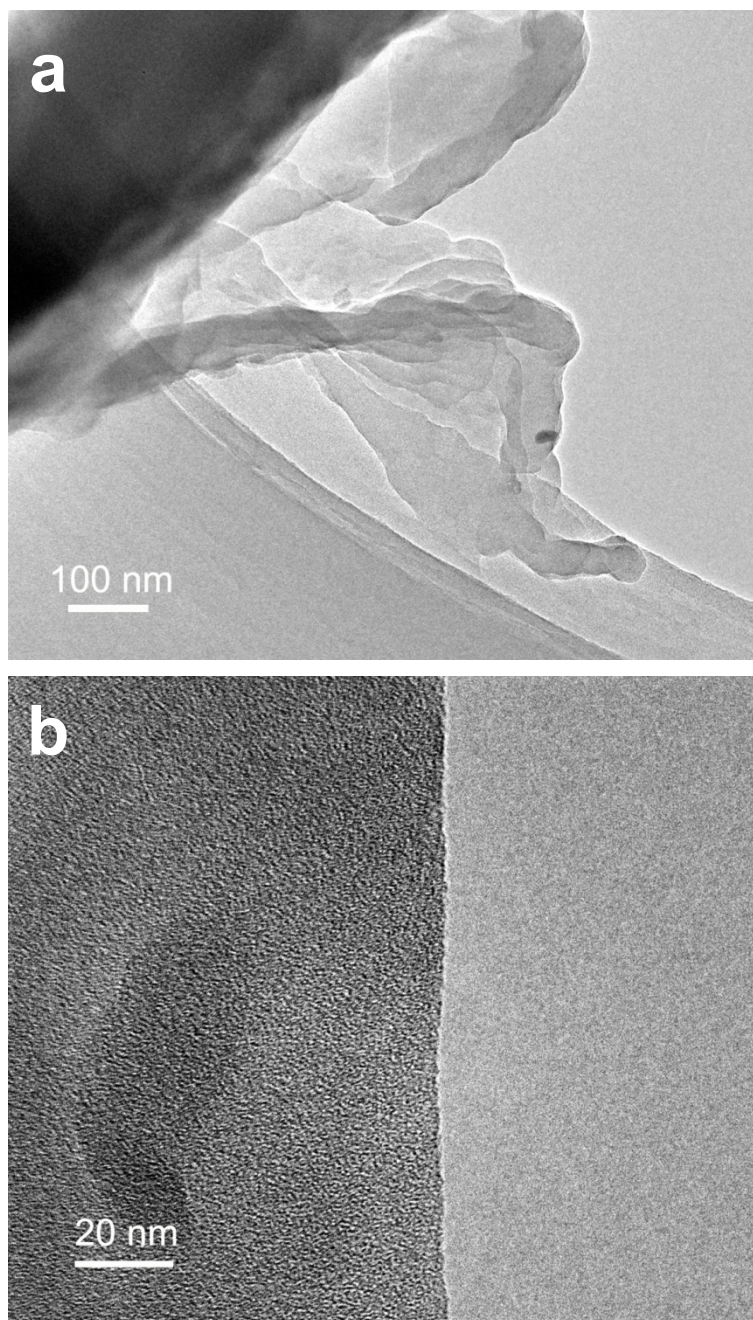
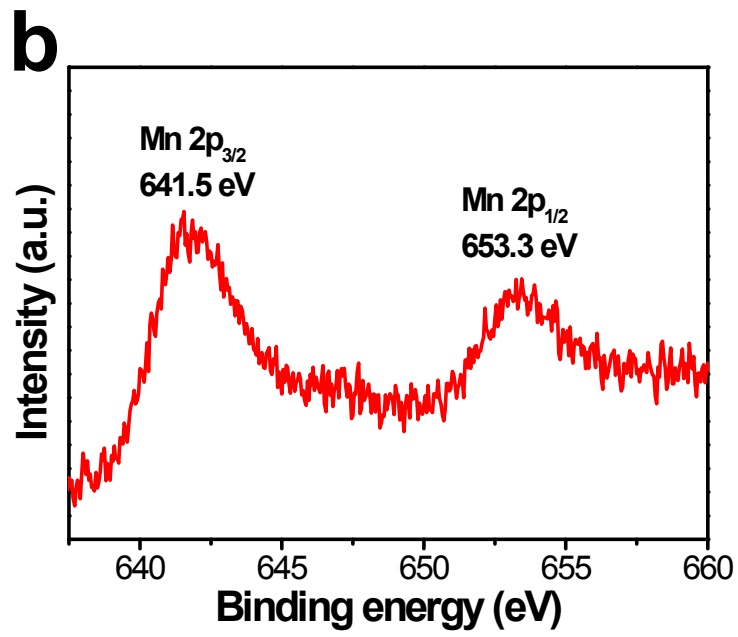
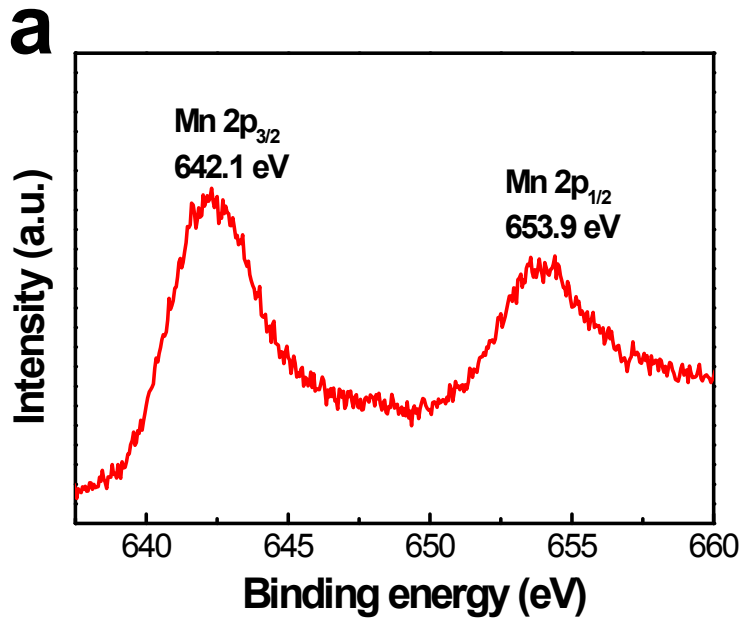


Figure S3: (HR)TEM images of natural CF with different enlargements (a and b). The natural CF's multiple layers could be observed from the images.



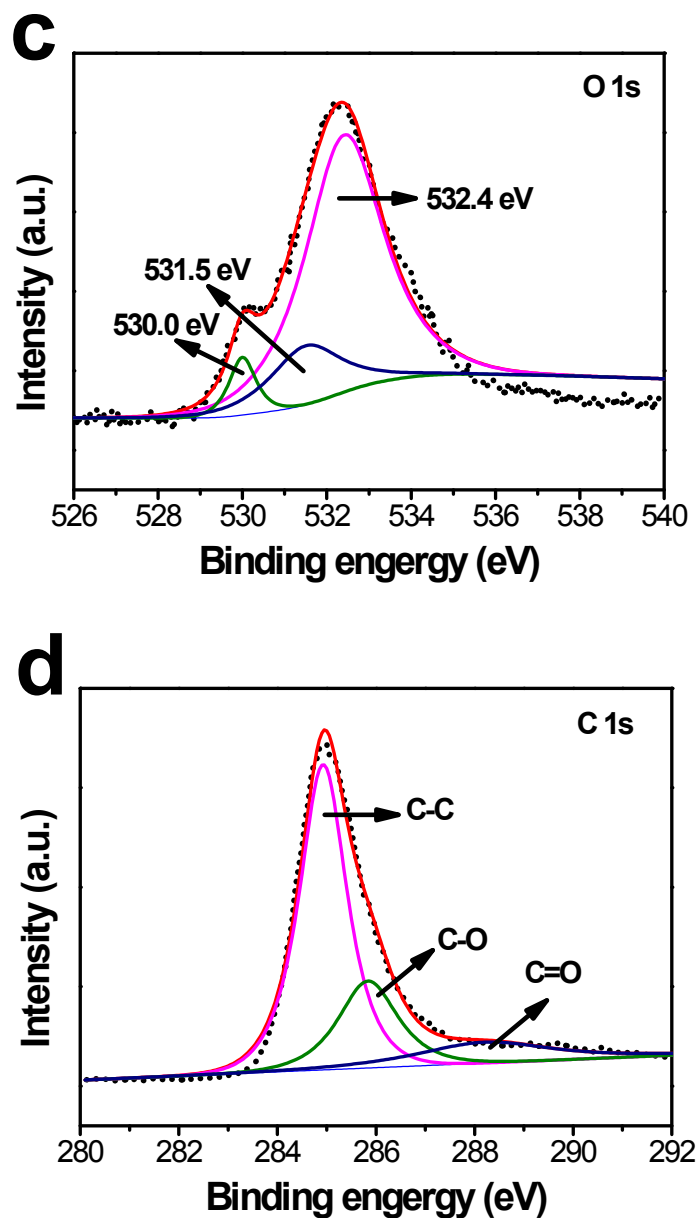


Figure S4: XPS spectrum of the MnO₂/CF precursor (a) and MnO/C sample (b-d). Two typical bands at 642.1 and 653.9 eV (a) is corresponding to the 2p_{3/2} and 2p_{1/2} orbits of Mn⁴⁺ of MnO₂, respectively. The two signals at 641.5 and 653.3 eV (b) may be attributed to Mn (II) 2p_{3/2} and 2p_{1/2} orbits, respectively, characteristic of MnO. The band at 532.4, 531.5 and 530.0 eV (c) can be assigned to the oxygen bond of C-OH phenol groups and/or C-O-C ether groups, Mn-O and C=O, respectively. A strong C 1s peak at 284.9 eV (d) corresponds to the graphitic carbon. The weaker one at 286.1 eV arising from the C-O, while the peak at about of 288.5 eV indicates the formation of C=O bonds.

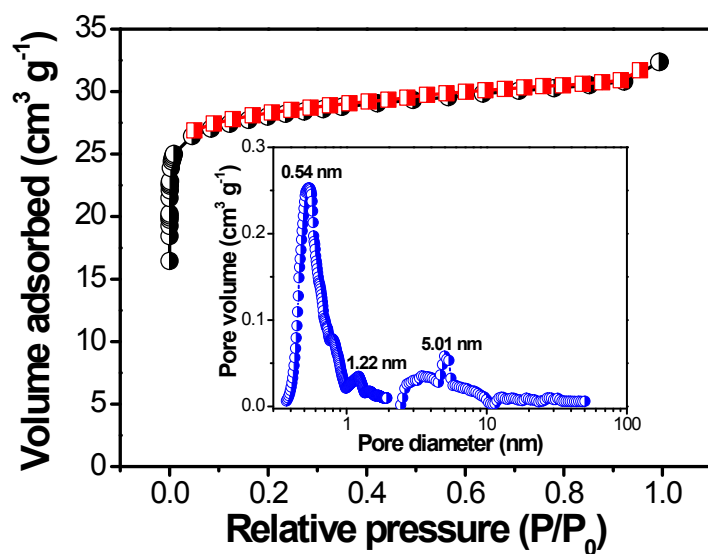


Figure S5: N₂ adsorption-desorption isotherms of the pure carbon. The insert is the pore size distribution curve calculated from the adsorption branch by the DFT model.

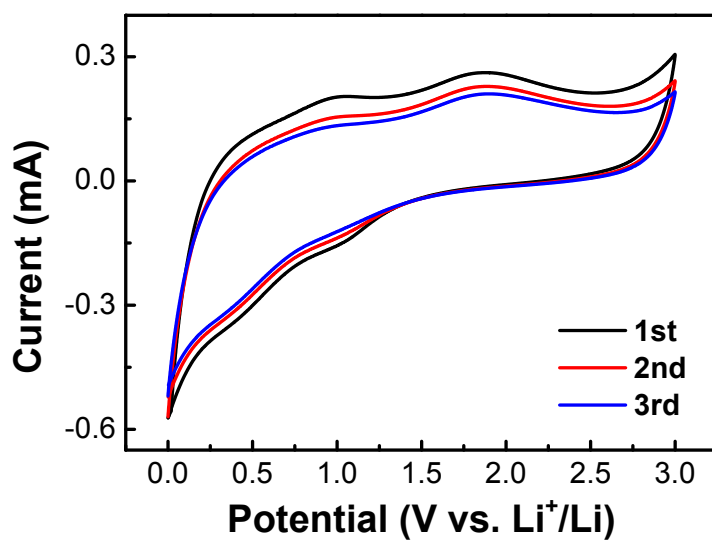


Figure S6: CV curves of the MnO/C sample at a scan rate of 1 mV s⁻¹.

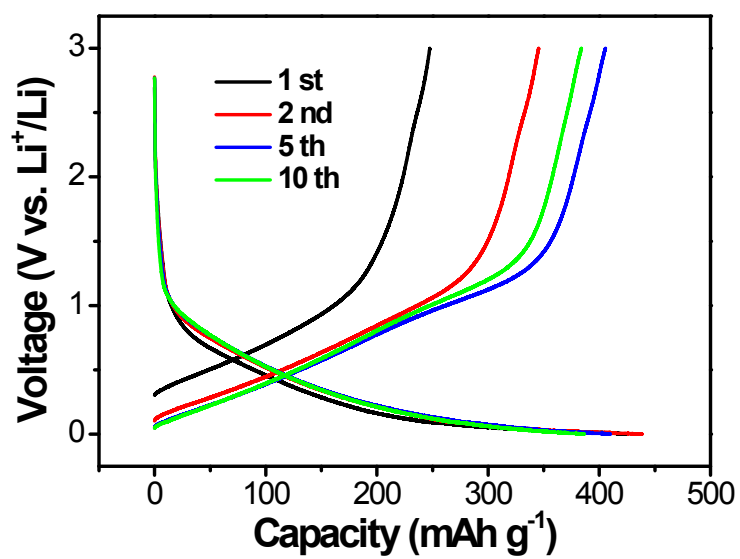


Figure S7: Charge-discharge profiles of the electrode containing pure carbon for cycles with a current density of 0.1 A g⁻¹.

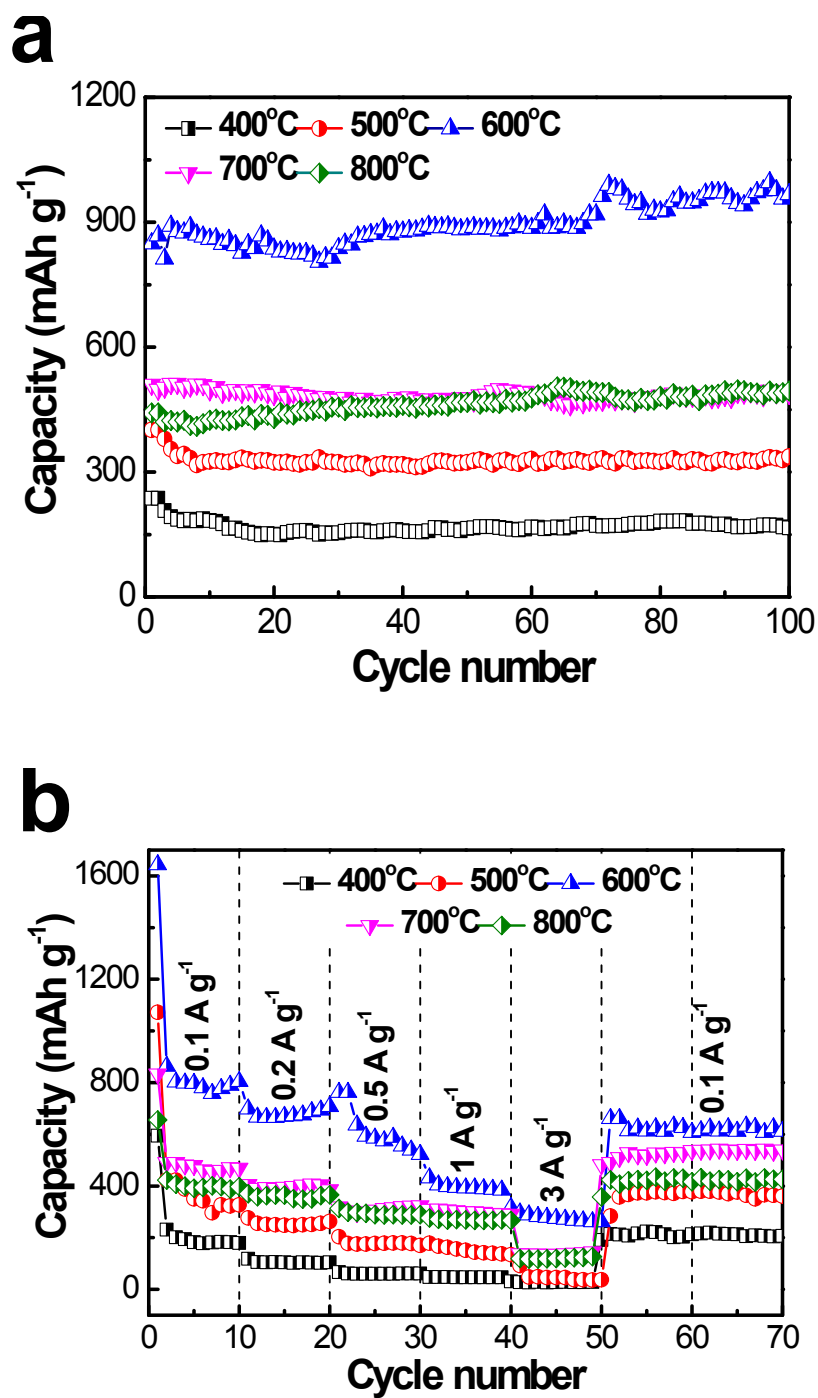


Figure S8: Cycling performance (a) and rate property (b) of the MnO/C electrodes with different calcination temperatures.

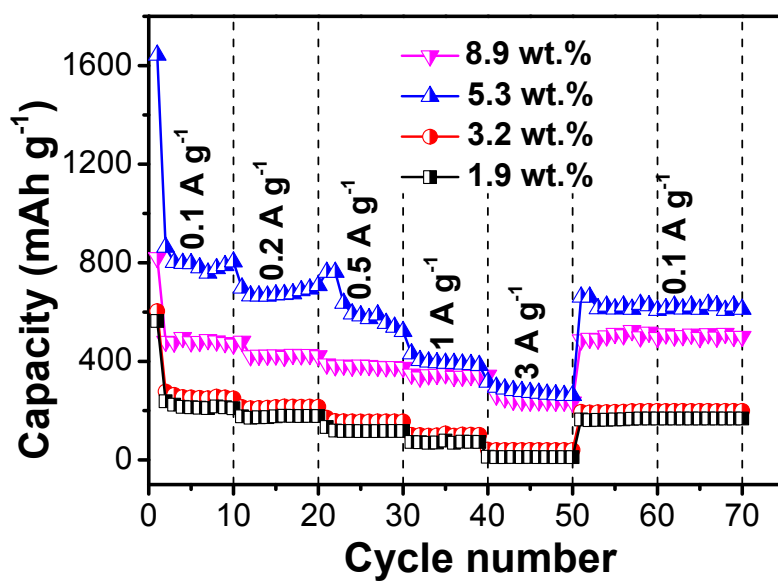


Figure S9: Rate performance of the electrodes containing MnO/C treated at 600°C with different MnO contents (1.9, 3.2, 5.3 and 8.9 wt.%).

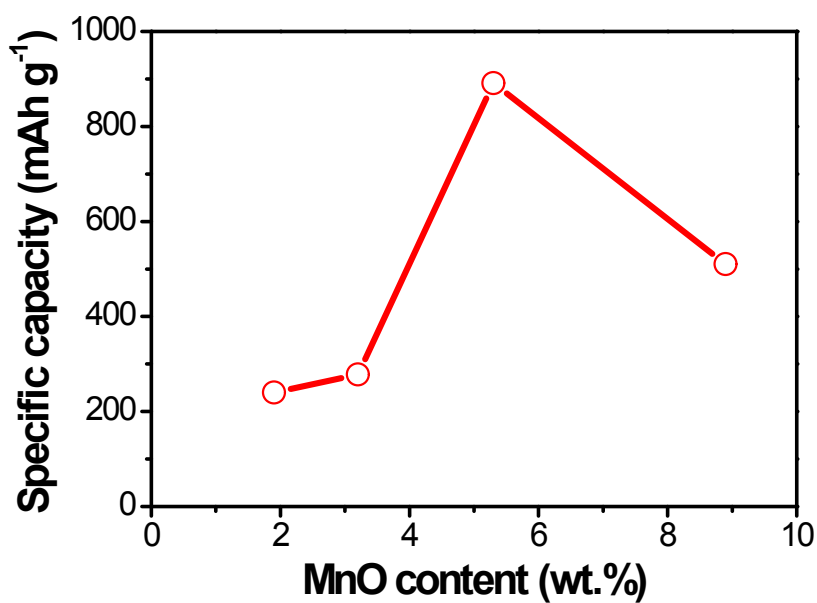


Figure S10: Specific capacity of the electrodes containing MnO/C treated at 600°C with different MnO contents (1.9, 3.2, 5.3 and 8.9 wt.%) at a current density of 0.1 A g⁻¹.

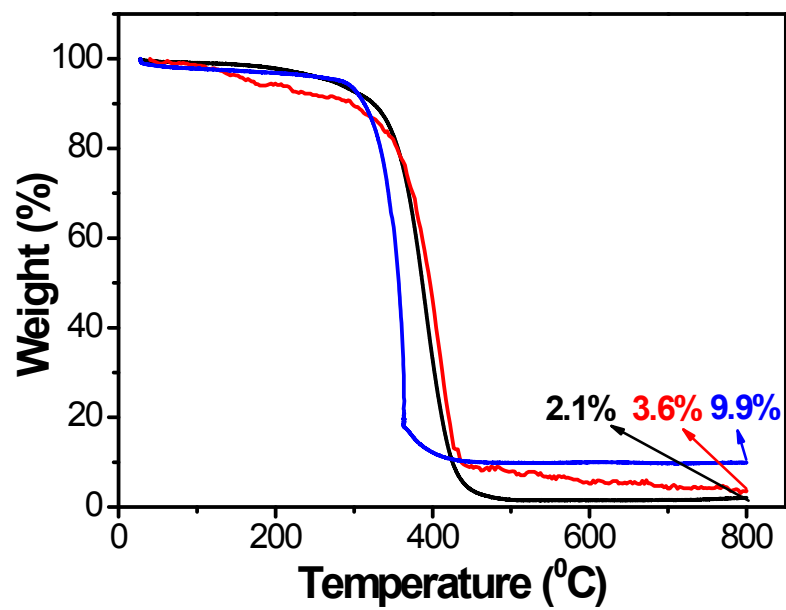
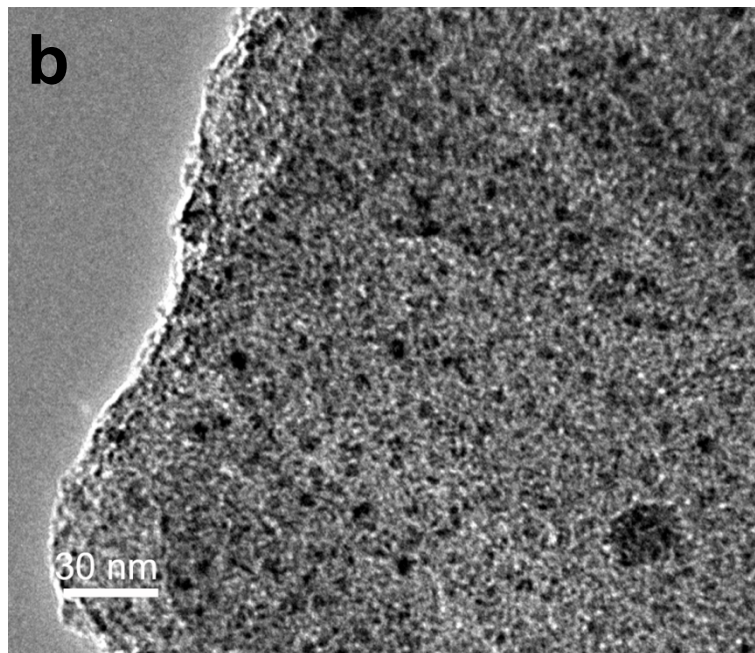
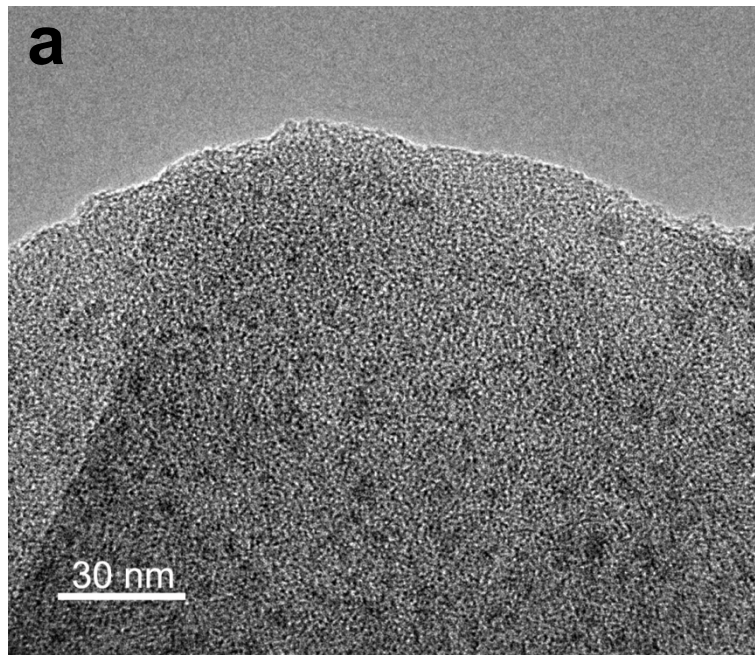


Figure S11: TGA curves of the electrodes containing MnO/C with different MnO contents (1.9, 3.2 and 8.9 wt.%)..



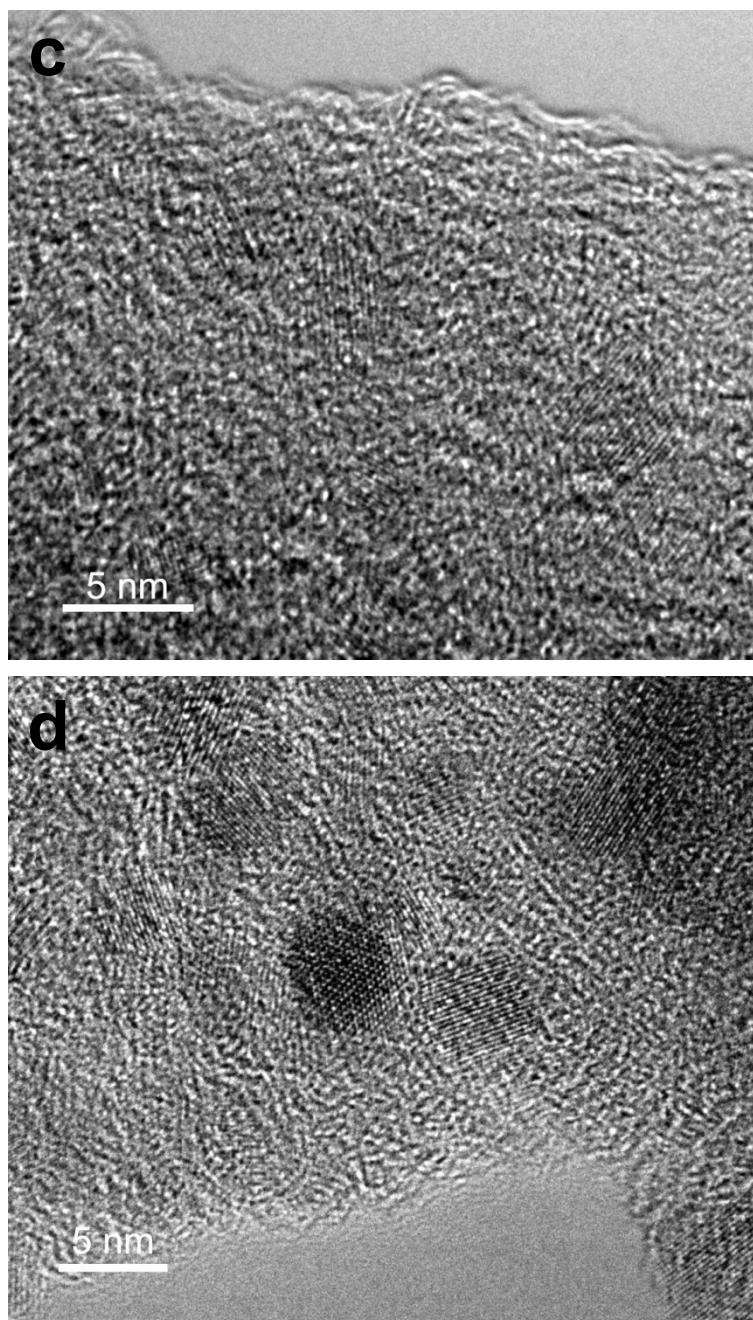


Figure S12: The HRTEM images of the MnO/C-1.90 (a and c) and the MnO/C-8.85 (b and d) samples.

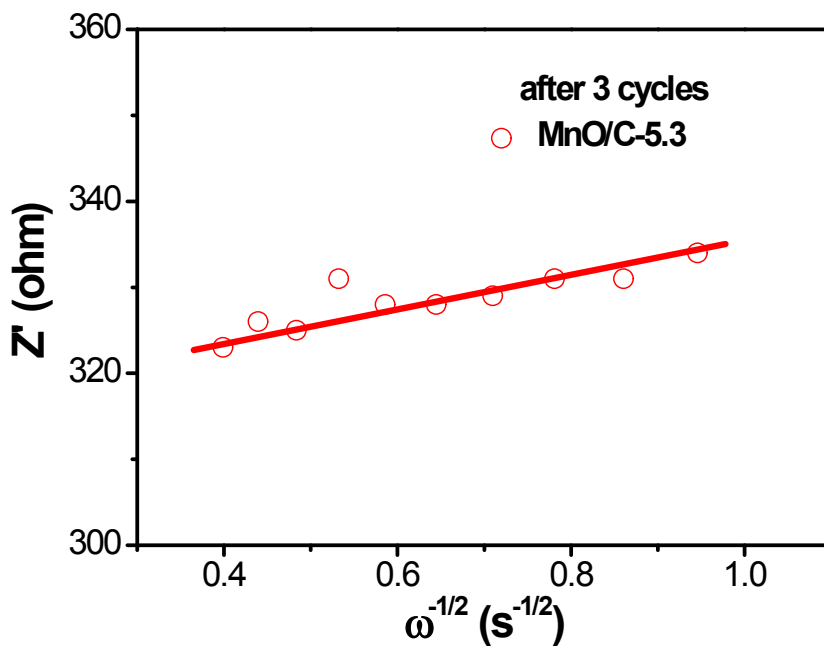


Figure S13: The relationship between Z' and $\omega^{-1/2}$ at low frequency for the MnO/C-5.3 after 3 cycles.

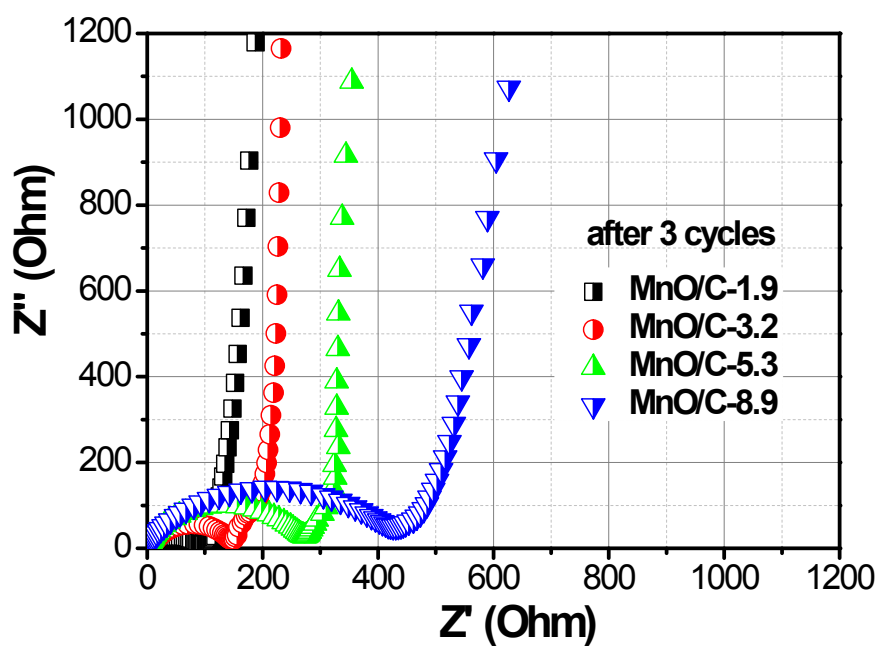


Figure S14: The Nyquist plots of the MnO/C electrodes with various MnO contents.

Table S1 Comparison of the MnO content, BET specific surface area and specific capacity of the MnO/C composite material by different methods.

Sample	MnO content [wt.%]	BET specific surface area [m^2g^{-1}]	First discharge specific capacity [mAh g^{-1}]	Specific capacity after X cycles at Y mA g^{-1} [mAh g^{-1}]	Reference
MnO/C nanotube	96.8	40.0	1129	763 (X=100,Y=100)	22
MnO/C nanowires	94.4	6.86	1196	801 (X=200,Y=100)	62
MnO@1-D carbon	89.4	-	1249	763 (X=100,Y=100)	31
MnO/C network	87.3	82.7	1456	1224 (X=200,Y=200)	63
MnO/Graphene	82.6	50.3	890	2014 (X=150,Y=200)	28
MnO/Microalgae	76.4	76.9	1021	702 (X=50,Y=100)	34
MnO/C-N web	76.3	-	1272	650 (X=100,Y=1000)	33
3D MnO/CNS	73.0	25.0	580	890 (X=500,Y=100)	36
MnO/C nanoplate	60.0	-	1265	563 (X=30,Y=200)	25
MnO/C nanocomposite	4.5	429.1	1620	952 (X=100,Y=100)	Our work

Table S2 Comparison of the resistance of electrolyte (R_s), the charge transfer resistance (R_{ct}) and diffusion coefficient (D) of the MnO/C composite sample with various MnO contents.

Sample	R_s [Ω]	R_{ct} [Ω]	σ_w [$\Omega \text{ cm}^2 \text{ s}^{-0.5}$]	D [$\text{cm}^2 \text{ s}^{-1}$]*
MnO/C-1.9	2.8	95	18.5	1.6×10^{-12}
MnO/C-3.2	2.8	148	17.2	1.9×10^{-12}
MnO/C-5.3	2.4	271	15.9	2.2×10^{-12}
MnO/C-8.9	3.7	431	24.2	9.5×10^{-13}

* $D = 0.5(R \cdot T / (A \cdot F^2 \cdot \sigma_w \cdot C))^2$, where R ($8.314 \text{ J K}^{-1} \text{ mol}^{-1}$) is the gas constant, T (298.5 K) is the Kelvin temperature, A ($\pi \times 0.5^2 \text{ cm}^2$) is the area of the electrode surface, F (96500 C mol^{-1}) is Faraday constant, C (1 mol) is the molar concentration of Li^+ ion, and σ_w is the Warburg coefficient. With Randles plotting, that is plotting Z' with $\omega^{-1/2}$ ($\omega = 2\pi f$) for a low-frequency Warburg response, the Warburg coefficient σ_w can be obtained by measuring the slope of such plots. The diffusion coefficient D of MnO/C-5.3 is the largest among the MnO/C-1.9, 3.2, 5.3 and 8.9 samples.

Notes

^aKey Laboratory of Bio-inspired Smart Interfacial Science and Technology of Ministry of Education, Beijing Key Laboratory of Bio-inspired Energy Materials and Devices, School of Chemistry and Environment, Beihang University, Beijing 100191, P. R. China. ^bBeijing Centre for Physical and Chemical Analysis, Beijing 100089, P. R. China. Correspondence should be addressed to Q. Gao. E-mail: qmgao@buaa.edu.cn. Tel: +861082338212. Fax: +861082338212.